High-field transport statistics and impact excitation in semiconductors

E. Bringuier
URA 800 du CNRS, Université Pierre et Marie Curie, Case 86, 4 place Jussieu, 75 252 Paris Cedex 05, France
(Received 2 November 1993)

The paper is devoted to the statistics of semiclassical charge transport in semiconductors subject to high electric fields. Two main approaches are distinguished: one is mostly analytical and makes use of the notion of a mean free path, and it led to the so-called lucky-drift model; the other one is based upon Monte Carlo computer simulations and has the ability to include a realistic band structure. The present paper aims to show that in spite of the differences in wording and viewpoint, both approaches are fundamentally equivalent. We first review the lucky-drift model in its simplest form, and then present some basic features of the statistical approach used in numerical simulations of transport. On the one hand, statistical concepts are introduced into the lucky-drift model, and the notion of lucky-drift trajectories is criticized and replaced by that of energy autocorrelation. On the other hand, the results obtained in numerical simulations are reproduced in the framework of a generalized lucky-drift model tailored to allow for strong nonparabolicities. The statistical description of transport is applied to the determination of the rate of inelastic collisions undergone by a hot electron in the presence of an impact-excitable impurity. It is argued that such a rate is a better indicator of the fraction of carriers attaining a certain energy than the band-to-band impact-ionization rate. The previous expression of the impact-excitation rate, derived on the basis of the picture of lucky-drift trajectories, is revised, and a comparison with experiment is attempted.

I. INTRODUCTION

There have been several approaches to the high-field transport regime in semiconductors, of which a review has been made by Capasso.[1] In very broad terms, two classes or traditions may be distinguished. The first is associated with the names of Wolff,[2] Shockley,[3,4] Baraff,[5] and Ridley,[6] to quote just a few: Their theories are based upon the notion of a mean free path for the hot electrons, and do not contain an explicit reference to the band structure, except for the carrier effective mass. The frameworks are analytical (Ridley's lucky-drift model reproduces Baraff's numerical curves) and are mostly concerned with the calculation of the band-to-band impact ionization rate. The second class of theories, introduced by Fawcett, Boardman, and Swain[7] and by Hess and co-workers,[8,9] is based upon Monte Carlo computer simulations including a realistic band structure: Such theories, which rest on the Boltzmann semiclassical transport equation, eventually modified to account for quantum effects,[9] describe in detail the electron trajectories in real and momentum space and allow the statistical calculation of all kinds of observables.[10] Both kinds of theories suffer from our limited knowledge of the electron-phonon interaction, as well as from the uncertainties in material parameters. Each kind of theory has its own merits: For example, the Monte Carlo simulations are potentially more accurate and give more detailed information about the transport, but they require running a computer program whenever a new situation arises, while the analytical theories rest on a simple physical picture allowing quick prediction of the chemical trends. Hence both classes of theories have to be used, depending on the question addressed in the contiguous realms of basic physics and device design. Ideally they should be employed in a complementary manner, but the discrepancies in viewpoint and wording are sometimes so great[1] that the frameworks almost seem mutually exclusive, which is very detrimental to a complete understanding of the phenomena under investigation. The aim of the present paper is to bridge the gap between both descriptions and allow a cross fertilization. On the one hand, we want to introduce some statistical-mechanical elements into the lucky-drift model developed by Ridley[6] and Burt[11,12] in order to extend its range of usefulness and warn against fallacious use of the so-called "lucky-drift trajectories." This is of immediate interest, since the model has become increasingly used in device modeling.[13–16] On the other hand, we aim at interpreting the numerical results of computer simulations in terms of the simple physical picture provided by the lucky-drift concept. This should facilitate the use of Monte Carlo–simulated results by nonspecialists. Above all, the aim is to establish a correspondence between both theories, so that each result obtained in one framework may receive further illumination when transposed into the other one. We are aware that some links between the two frameworks have already been set up. Indeed it was Shichijo and Hess's numerical work,[8] showing that drifting electrons prevailed in the high-energy tail of the hot-electron distribution, that triggered Ridley's elaboration[6] of the lucky-drift model. And McKenzie and Burt[12] used a Monte Carlo simulation to support Burt's variant[11] of the lucky-drift model. However, the links between both classes of theories are not always well or completely un-

derstood, thereby preventing the conjugate use of both viewpoints. In clarifying the existing relationships we hope to show that they are in fact much stronger than is commonly felt. The approach adopted herein is heuristic and tentative in part, but important qualitative results are obtained in an almost calculationless manner. Where analytical calculations could not be done *in extenso,* scaling shortcuts have been used, the justification of which lies in the consistency of the whole picture.

Section II is devoted to transport statistics, not to the microscopic quantum processes governing the electron-lattice interaction. It is structured as follows. Subsection A sets out the gist and the main results of the lucky-drift approach to the high-field transport regime in the well-understood case of parabolic bands. This will, *inter alia,* provide us with a language allowing us to formulate questions and thereby start a dialogue with the other class of theories. Subsection B deals with the statistical framework employed in Monte Carlo numerical models. Only those elements (distribution function and averages) which are necessary for our later purpose are recalled. Then Subsec. C attempts a reinterpretation of the lucky-drift model in the light of the picture emerging from the simulations. This in turn provides simple relationships expected to hold in arbitrary numerical simulations, at least in an approximate manner. Subsection D illustrates the new statistical picture with the notions of drift and diffusion. In Subsec. E we examine the behavior of the lucky-drift model in an arbitrary band structure, with special interest in the multivalley case.

In Sec. III the new statistics is applied to revise a previous calculation[15] of the hot-electron impact excitation rate of an impurity capable of undergoing internal transitions, whose physical significance has been largely underestimated so far in spite of its well-known technological interest.

Before entering Sec. II, a word of caution is necessary. In the literature, two distinct subjects have often been mingled, namely, high-field transport and band-to-band impact ionization.[1] The usual test of high-field transport theories has long been through the experimentally measured impact-ionization rate per unit length (α_n for electrons). This assumed (sometimes implicitly) that once a carrier had reached the threshold energy for lattice ionization, E_i, hole-electron pair creation took place immediately, so that the impact rate was straightforwardly related to the fraction of carriers reaching E_i. That hypothesis is called the "hard-threshold" assumption. It is now widely recognized that the threshold is "soft":[1,17,18] The probability of impact ionization is low in the vicinity of the energy-momentum threshold E_i, so that (i) pair creation hardly affects transport beyond E_i; and (ii) the number of hole-electron pairs created is not simply related to the fraction of electrons attaining E_i. In a number of previous works, the results are cast in terms of the impact-ionization rate, and one has to isolate the results regarding transport from assertions on the very phenomenon of impact ionization. In the present paper, Sec. II deals with transport only, and Sec. III suggests an alternative indicator of the fraction of carriers attaining a certain energy.

II. TRANSPORT STATISTICS

A. The lucky-drift model

The lucky-drift model was introduced by Ridley[6] in 1983 as an extension and improvement of Shockley's lucky-electron model.[4] Its motivation comes from the numerical works of Baraff[5] and of Shichijo and Hess.[8] The former considers a parabolic band structure, and the (nonpolar) electron–optical-phonon interaction (following Shockley) is characterized by a constant mean free path λ. The latter work considers a realistic band structure, obtained from pseudopotentials, and the electron-phonon interaction (both polar and nonpolar) is treated according to first-order perturbation theory in which the matrix elements are taken at the high-symmetry points. In those two numerical works, the vast majority of electrons reaching the ionization threshold energy do so by drift, not ballistically as Shockley supposed. Thus the probability $\exp(-E/qF\lambda)$ for a collisionless flight up to energy E in an electric field F largely underestimates the number of electrons reaching E. Ridley[6] argued that, because at high energies the energy relaxation time largely exceeds the mean free time, it is possible for an electron to attain energy E while drifting in the field. Indeed the associated probability of "lucky drifting" to energy E is higher than the probability of attaining E in a ballistic flight. This explains Baraff's curves quantitatively and Shichijo and Hess's results qualitatively.

The lucky-drift model was subsequently clarified and further established by Burt[11] and McKenzie and Burt.[12] They performed[12] a Monte Carlo simulation of high-field transport in a model semiconductor characterized by a parabolic band structure where the deformation-potential electron-phonon interaction has a constant mean free path, in accordance with Baraff's work. In this simple case the lucky-drift model is fully analytical, and the comparison with the numerical simulation provided a test of the model. The probability for the electron to reach some given energy (say, the ionization threshold energy E_i) such as given by the simulation was accurately reproduced by the lucky-drift model over four orders of magnitude, without using disposable parameters.

We shall recall here some of the basic hypotheses and results of the model which will be of direct concern in the following. For more details the reader is referred to Refs. 6, 11, and 12. Let us first rederive the probability $P(E)$ for an electron to reach energy E in the presence of a field F. $P(E)$ is thought of as the probability of traveling a distance $z=E/qF$ downfield, starting from $z=0$, *without* relaxing energy to the lattice. While moving from $z=0$ to $z=E/qF$, the electron continuously gains energy from the field. Energy relaxation is modeled by artificial energy-relaxing events in which the electron loses all its energy suddenly. The link with reality is that the time rate at which energy is relaxed is the true physical expression (also employed in Monte Carlo simulations) in which the electron-lattice scattering rate is obtained from the golden rule including the relevant matrix element.

There are two transport modes for a carrier: (i) in the ballistic mode, characterized by the mean free path λ and the mean free time τ, the electron does not relax momen-

tum nor energy; (ii) in the drift mode, which takes place once the electron has suffered one collision, energy relaxation is characterized by a relaxation length λ_E. That length is the product of the energy relaxation time $\tau_E(E)$, defined by

$$E/\tau_E=\hbar\omega/[2n(\omega)+1]\tau\ , \tag{1}$$

(where $\hbar\omega$ is the optical phonon energy, $n(\omega)=[\exp(\hbar\omega/kT)-1]^{-1}$ is the Bose-Einstein number, and $\hbar\omega/[2n(\omega)+1]$ is the average energy lost by the electron in an electron-phonon collision), and of the drift velocity $v_d(E)$ of an electron of energy E:

$$v_d(E)=qF\tau(E)/m^* \tag{2}$$

(where m^* is the effective mass). This assumes that the momentum significantly varies during a collision, or in other words that the momentum relaxation time is close to the collision time τ. This condition is obeyed in nonpolar semiconductors, and in polar materials at sufficiently high fields where nonpolar coupling prevails. Just like λ, $\lambda_E=v_d(E)\tau_E(E)$ is independent of energy in the case of spherical parabolic bands and deformation-potential electron-phonon interaction. For the lucky-drift concept to be valid, λ_E must be much larger than λ, which becomes true at high enough fields for wide-gap semiconductors in which the dominant energy loss to phonons is via the nonpolar interaction. The two lengths are related through:

$$\lambda_E=\frac{1}{2}\frac{qF\lambda}{\hbar\omega/[2n(\omega)+1]}\lambda\ , \tag{3}$$

so that $\lambda_E\gg\lambda$ if the energy gained over a free path is much larger than the average energy lost per collision. Since $\lambda_E\sim F$, this should occur at high enough F.

The probability $P(E)$ is the sum of two terms. Either the electron escapes lattice interaction (over a spatial scale $\sim\lambda$), or it is deflected and then enters a state of drift associated with the energy relaxation length λ_E. The first term is Shockley's probability of no collision, $\exp(-E/qF\lambda)$. The second one refers to an electron which has collided once and then drifts. Consequently

$$P(E)=\exp(-z/\lambda)+\int_0^z\exp(-z'/\lambda)(dz'/\lambda)\times\exp[-(z-z')/\lambda_E]\ , \tag{4}$$

where z' is the distance at which the electron begins to drift. The structure of the second term in the right-hand side of Eq. (4) is transparent: (i) the electron travels ballistically from $z=0$ to z', with a probability $\exp(-z'/\lambda)$; (ii) it has a probability dz'/λ of interacting with the lattice between z' and $z'+dz'$, thereby effecting the transition to the drift mode; (iii) finally in that mode it has a chance $\exp[-(z-z')/\lambda_E]$ of avoiding energy relaxation up to $z=E/qF$. In the remainder of the paper z will be called the lucky-drift variable.

The integration in (4) is straightforward:

$$P(E)=\exp(-E/qF\lambda)+\frac{\exp(-E/qF\lambda_E)-\exp(-E/qF\lambda)}{(1-\lambda/\lambda_E)}\ . \tag{5}$$

The result has been examined in detail by McKenzie and Burt,[11,12] and the hard-threshold ionization rate α_n derived therefrom is in excellent agreement with a numerical simulation.[12]

We list and comment on two other results obtained in this model. Consider first the average energy $E_{\rm av}$. The calculated value $qF(\lambda_E+\lambda)\simeq qF\lambda_E$ scales like F^2. This is a direct consequence of the parabolic-band density of states, which entails a scattering rate $1/\tau(E)\sim E^{1/2}$. If the energy-balance equation

$$qFv_s=\frac{\hbar\omega}{2n(\omega)+1}\left\langle\frac{1}{\tau}\right\rangle \tag{6}$$

is written in the saturation region, i.e., with a field-independent drift velocity v_s, and if $\langle 1/\tau\rangle\simeq 1/\tau(E_{\rm av})$ (apart from a dimensionless factor close to unity), then $E_{\rm av}\sim F^2$.

As a second example, we consider the average drift velocity. It is taken[12] to be $v_d(E_{\rm av})$, whence:

$$v_s=\{\hbar\omega/[2n(\omega)+1]m^*\}^{1/2}\ , \tag{7}$$

whatever the electric field, i.e., it is the drift velocity at saturation v_s. Equation (7) is just what would be obtained from energy and momentum balance assuming a monoenergetic distribution,

$$m^*v_d=qF\tau\ , \tag{8a}$$

$$qFv_d=\hbar\omega/[2n(\omega)+1]\tau\ . \tag{8b}$$

[Strictly speaking, in Eq. (8a) we have replaced the momentum relaxation time by the collision time τ, as is customary.] Those equations entail (7). The constancy of the drift velocity has a natural explanation in the lucky-drift picture: Momentum relaxation is so strong that any increase in $\langle\hbar\mathbf{k}\rangle=\langle m^*\mathbf{v}_d\rangle$ is prevented, while the larger space-time scales for energy relaxation allow $E_{\rm av}$ to increase with F.

B. The energy distribution function

The statistical description which is used in the numerical simulations depends on the electron population as a function of the energy E above the bottom of the conduction band E_c taken as the zero energy. The density of available conduction states per unit energy interval and per unit volume $N(E)$ may in principle be obtained from the crystalline structure. The states can be more or less occupied, and this is quantified by the occupation function $f(E)$ varying between zero and unity. The total number of electrons per unit volume in the conduction band is thus:

$$n_e=\int_0^{+\infty}N(E)f(E)dE\ , \tag{9}$$

where $+\infty$ stands for the top of the conduction band. Denoting by $n(E)dE$ the *fraction* of electrons between E and $E+dE$, we have:

$$n(E)=N(E)f(E)/n_e \tag{10}$$

and $n(E)dE$ is also the probability for an electron to have its energy lying between E and $E+dE$.

In the numerical simulations of high-field transport, an electron is introduced at zero energy, and then experiences heating in a field F and cooling to the phonons according to the collision rates of the various electron-phonon interactions. For an overview of the Monte Carlo procedure see Refs. 7 and 12, and Ref. 19 for a detailed account. After some time, a steady-state regime is achieved in which the electron energy E fluctuates around a well-defined average energy E_{av}. If the simulation is repeated over a large number of particles, the number of carriers whose energies lie between E and $E+dE$ after a given time is a measure of $n(E)$. Then the ensemble average of each one-particle energy-dependent observable $A(E)$ may be calculated through the formula:

$$\langle A \rangle = \int_0^{+\infty} A(E) n(E) dE \ . \tag{11}$$

It should be noted that the description of the electron population through $n(E)$ is not complete. The quantum state of an electron is defined by its crystal momentum $\hbar\mathbf{k}$ and its spin (the latter being insensitive to the electron-phonon interaction). Where anisotropy plays a role, knowledge of the wave vector is important. This will be considered briefly in Sec. III on a special example. The discussion is here restricted only to the distribution of electrons in the energy space. Note that when electrons are present in high-energy valleys of the conduction band(s), $\hbar\mathbf{k}$ and the spin are not sufficient to specify the electron state any more; the energy E should be given, too.

In the lucky-drift approach, an electron is introduced in an electric field F at zero energy, and the probability $P(E)$ for the electron to reach energy E from the field F in spite of inelastic phonon scattering is computed. Since $P(E)$ is the probability that the electron reaches energy E or more,

$$P(E) = \int_E^{+\infty} n(E') dE' \ , \tag{12}$$

or equivalently:

$$n(E) = -(dP/dE) \ . \tag{13}$$

The energy distribution $n(E)$ for the simplest lucky-drift model [constant λ and λ_E, Eq. (5)],

$$n(E) = \frac{\exp(-E/qF\lambda_E) - \exp(-E/qF\lambda)}{qF(\lambda_E - \lambda)} \ , \tag{14}$$

is shown in Fig. 1. The maximum is located at $E = qF\lambda(1-\lambda/\lambda_E)^{-1}\ln(\lambda_E/\lambda)$, that is, at some $qF\lambda$. At high energy $n(E)$ decays as $\exp(-E/qF\lambda_E)$.

In deriving $P(E)$ it is considered that the probability for a drifting electron not to relax energy to the lattice (that is, to merely acquire electric potential energy from the field) is $\exp\{-\int dt'/\tau_E[E(t')]\}$. Energy relaxation to the lattice occurs abruptly, i.e., the electron loses all its energy in an "energy-relaxing event." This approach is a generalization of Shockley's lucky-electron model, and is reminiscent of the Drude model of conductivity, where an electron loses all its momentum in a collision. Because in Eq. (1) τ_E is defined so as to give the correct energy loss to the lattice, the electron energy distribution is correctly reproduced by Eqs. (5) and (13), which entail Eq. (14). The definite proof that the approach is basically sound in deriving $P(E)$ has been given by McKenzie and Burt in their Monte Carlo simulation in a model semiconductor of parabolic band structure.[12]

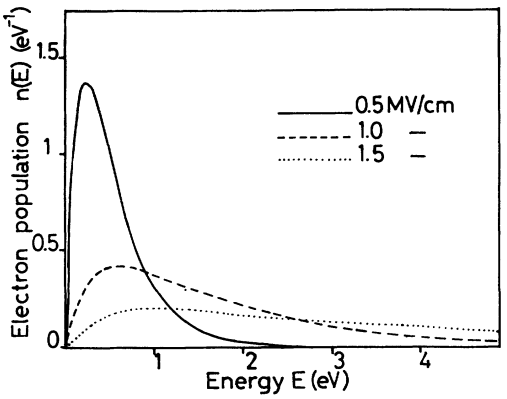

FIG. 1. Normalized electron population $n(E) = -dP/dE$ (in eV^{-1}) of the lucky-drift model in parabolic bands at several fields F ($\lambda = 30$ Å, $\hbar\omega = 42$ meV, $m^* = 0.30 m_0$, $T = 300$ K).

The so-called lucky-drift trajectories (i.e., E vs z) show continuous energy increase followed by abrupt relaxation to the zero energy (bottom of the conduction band). Clearly this is a mathematical device which correctly reproduces the hot-electron behavior *in the energy space,* but not a physical picture of the true trajectories. Actually the electron energy changes by $\pm\hbar\omega$ in one electron-phonon interaction. The correct picture is that of an average energy E_{av} given by

$$E_{av} = \int_0^{+\infty} E(-dP/dE) dE \ , \tag{15}$$

around which the electron energy fluctuates in time according to the distribution function $n(E)$. More precisely, the ergodic principle tells us that in the steady-state regime the fraction of time spent between E and $E+dE$ is $n(E)dE$. The expectation value of a one-particle, energy-dependent observable $A(E)$ should *not* be calculated with the assumption that the lucky-drift trajectories reflect the evolution of energy in real space and subsequently perform an average over such a trajectory. Rather, $\langle A \rangle$ should be calculated in the standard manner of statistical mechanics, viz., through Eq. (11). An example will be treated in detail in Sec. III.

C. The energy correlation length

Artificial though they may appear, the energy-relaxing events invoked in the lucky-drift picture have a deep, unsuspected significance. Because, in such an event, the energy is reset to zero, just after the event the electron has lost all memory of its previous motion altogether. The electron experiences a series of loss-free acceleration bursts which are independent of each other. In between two "unlucky" (that is, energy-relaxing) collisions, the energy values are correlated: if l_c denotes the average length drifted between two unlucky events, and if the electron travels downfield over a length $l \gg l_c$, it is very

unlikely that no energy-relaxing collision has occurred in between, so that the energy values are uncorrelated over a length l. Thus l_c has the meaning of a correlation length; this is further substantiated in the Appendix by means of a spatial Langevin approach to the transport in the drift regime, in which the carrier energy stochastically oscillates around the average energy due to random exchange of phonons with the lattice. The value of l_c may be readily obtained from the lucky-drift picture. The energy gained over l_c is qFl_c, and since l_c is the average distance drifted downfield between energy-relaxing events, qFl_c is the average electron energy $E_{\rm av}$ defined by Eq. (15). Hence the correlation length is:

$$l_c = E_{\rm av}/qF \ . \tag{16}$$

In the Appendix it is argued that such a picture is of general significance, and not restricted to the lucky-drift framework, and a more general definition of l_c is given. That length may be viewed in a different manner: it is that over which the energy can take all values according to the distribution function $n(E)$. For a given field F, there is an average energy $E_{\rm av}$, around which the instantaneous energy fluctuates on the scale of the correlation length; E takes virtually any value over a distance l_c.

We are now in a position to describe the evolution of energy versus drifted distance in a realistic manner, more akin to that observed in the Monte Carlo simulations, see Figs. 16 and 17 of Ref. 8, while retaining the handy lucky-drift framework. Let E_0 be some definite energy: $P(E_0)$ is the probability for the actual electron energy E to be E_0 or more; $1-P(E_0)$ is the probability that $E<E_0$. We now ask the following question: If at some given point of space $E<E_0$, what is the probability [denoted by $P_<(E_0,l)$] that E stay below E_0 during a length l? As E fluctuates along the electron path, for large l it becomes increasingly unlikely that E always keeps below E_0. We divide l into $n=l/l_c$ segments equal to the correlation length. Over each segment l_c, the electron virtually explores the available energy range, with a probability $1-P(E_0)$ to remain below E_0. Considering that each segment is uncorrelated with the others, the probability $P_<(E_0,l)$ that E always stays below E_0 may be factorized into:

$$[1-P(E_0)]^n = \exp\{l\ln[1-P(E_0)]/l_c\} \ . \tag{17}$$

It can be written as:

$$P_<(E_0,l) = \exp[-\alpha_<(E_0)l] \ , \tag{18}$$

where

$$\alpha_<(E_0) = -\ln[1-P(E_0)]/l_c \tag{19}$$

appears as the probability per unit length that E exceeds E_0, which is vanishingly small for high energies. To check that this expression makes sense, let us examine two limiting forms. First, for $E_0 \gg E_{\rm av}$, $P(E_0)$ is small, and (19) reduces to:

$$\alpha_<(E_0) = P(E_0)/l_c \ , \tag{20}$$

so that $\alpha_<(E_0)$ is proportional to the probability that E exceeds E_0, which looks satisfactory. In fact Eq. (20), with l_c given by (16), is identical to Burt's expression[11] for the impact ionization rate with E_0 as the (hard) threshold energy for pair production. The comparison with Burt's model[11] is possible because $E_{\rm av} \ll E_0$: Hence hard-threshold impact ionization negligibly modifies Burt's statistics in cutting off the energy distribution beyond E_0.

Expression (20) is not valid at low energies [$E_0 \ll E_{\rm av}$, $P(E_0) \simeq 1$]: it would give a finite probability, while it is extremely unlikely for a particle to stay near zero energy under high-field conditions. The exact expression (19) yields $\alpha_<(E_0) \to +\infty$, and $P_<(E_0,l) \to 0$, in agreement with physical intuition.

At this stage the artificial character of the lucky-drift trajectories is evident. In that picture, the electron repeatedly returns to zero energy, while in actuality it spends most of its time where $n(E)$ is highest, that is, not far from $E_{\rm av}$. From the ergodic principle the fraction of time spent at energies between 0 and E_0 is $1-P(E_0)$. It vanishes as $E_0 \to 0$ [indeed $1-P(E_0)$ is *quadratic* in E_0 near zero according to Eq. (5)]. This is also what Eq. (19) tells us. Hence the collisionless trajectories envisaged in lucky-drift theory simply are a mathematical trick allowing the calculation of $P(E)$. They have no physical reality and can lead to erroneous conclusions when used outside their realm, namely, in the determination of the electron energy distribution $n(E) = -dP/dE$.

As for $P_<(E_0,l)$, we may calculate the probability $P_>(E_0,l)$ that a particle starting with energy $E>E_0$ remain above E_0 after a distance l. We find

$$P_>(E_0,l) = \exp[-\alpha_>(E_0)l] \ , \tag{21a}$$

with

$$\alpha_>(E_0) = -\ln P(E_0)/l_c \ , \tag{21b}$$

and a similar interpretation holds. The limiting form of Eq. (21b) for low energies [$P(E_0) \simeq 1$] is

$$\alpha_>(E_0) \simeq [1-P(E_0)]/l_c \to 0 \ , \tag{22}$$

and $P_>(E_0,l)$ departs from unity for distances l much in excess of the correlation length. In other words, it takes a lot of length for the particle to move down to low energies ($E<E_0$).

The above reasoning is valid over length scales $l \gg l_c$, or, better said, the typical lengths $\alpha_<^{-1}$ (after which E overtakes E_0) and $\alpha_>^{-1}$ (after which E drops below E_0) should exceed the correlation length l_c. Nevertheless, in spite of that limitation in the use of the rates $\alpha_<$ and $\alpha_>$, which should be much less than l_c^{-1}, they may give acceptable results for $\alpha_< l_c$ or $\alpha_> l_c$ approaching unity. To illustrate this, let us determine the energy E_0 which is most frequently crossed. The number of E_0 crossings per unit length is $\alpha_<(E_0)+\alpha_>(E_0) = -l_c^{-1}\ln\{P(E_0)[1-P(E_0)]\}$. It is maximum for $P(E_0)=\frac{1}{2}$: E_0 can be viewed as the demarcation energy $E_{1/2}$, with 50% of the electrons above the energy $E_{1/2}$, and 50% below. Thus even though for that value $\alpha_< l_c$ and $\alpha_> l_c = \ln 2$ approach unity, the conclusion is at least qualitatively right. In

practice, $E_{1/2}$ lies close to E_{av} if the distribution is well behaved. We recover the conclusion that the electron spends most of its length around E_{av}, and not at zero energy as the lucky-drift trajectories erroneously suggest. In the same way, note that if E_0 stands below the demarcation energy [i.e., $P(E_0) > \frac{1}{2}$], $\alpha_<(E_0) > \alpha_>(E_0)$, the drift along the field will make the electron's energy cross E_0 upwards more frequently than downwards. Hence the random collisions tend to bring the electron's energy near the demarcation level, around which the carrier energy stochastically oscillates.

We can obtain more from the simple reasoning leading to Eq. (17). Considering a particle of initial energy $E < E_0$, we have found the probability that over a distance l the energy *never* overtakes E_0. It is $\exp(-\alpha_< l)$, and $\alpha_<(E_0)$ is the probability per unit length for the energy to exceed E_0. Over a large distance ($l \gg l_c$), the number of times E crosses E_0 upwards is thus $\alpha_<(E_0)l$. We next ask: What is the probability $P_{up,1}$ that the energy goes *once* above E_0? As the probability per unit distance $\alpha_<(E_0)$ is constant if we look at a scale greater than l_c, we may use Poisson statistics and write down $P_{up,1}$ as

$$P_{up,1} = \alpha_<(E_0) l \exp[-\alpha_<(E_0) l] \ . \tag{23}$$

The use of Poisson statistics is justified for independent (i.e., uncorrelated) events occurring with a constant probability per unit time (in the case of photon counting) or per unit length (in the present case of particle motion). Here it is justified provided that the average length $\alpha_<^{-1}$ separating two events (viz., E_0 crossing towards higher energies) be larger than the correlation length, viz., $\alpha_<(E_0) l_c \ll 1$. This will hold for low values of $P(E_0)$, that is, improbably high energies. Similarly, the probability that over a distance l the electron overtakes n times the energy E_0 is

$$P_{up,n} = [\alpha_<(E_0) l]^n \exp[-\alpha_<(E_0) l]/n! \tag{24}$$

For improbably low energies E_0 [i.e., $P(E_0) \to 1$], we can calculate accurately the probability that it be reached n times downwards while traveling over a distance l:

$$P_{down,n} = [\alpha_>(E_0) l]^n \exp[-\alpha_>(E_0) l]/n! \tag{25}$$

D. Drift and diffusion

Drift is the result of momentum averaging through lattice scattering. Let us try to envision the time evolution of crystal momentum $\hbar\mathbf{k}$ in the way we described the behavior of energy. Whether in the lucky-drift picture or in a Monte Carlo simulation, between two (momentum-relaxing) collisions the evolution of $\hbar\mathbf{k}$ is deterministic, and after each collision the memory of the previous momentum state is destroyed. This again suggests that momentum values are correlated over a time τ, the collision time, which is approximately equal to the momentum relaxation time, and this is readily confirmed by a classical Langevin approach (by "classical" we mean that the evolution is described with time as the variable). It is worthy of remark that the momentum correlation time $\tau(E)$ depends on the energy state of the particle. This comes about because a collision changes the energy by $\pm\hbar\omega \ll E$, while it changes the momentum altogether, so that the hot electron explores a constant-energy surface $E(\mathbf{k})$ in $\mathbf{k}$ space over time scales of some τ. Energy evolves over larger times $\sim\tau_E(E)$.

We have schematically described momentum correlation in time. What about space? In terms of the path actually traveled by the particle, the correlation extends over λ, the mean free path. If we consider the drift variable x, the momentum correlation length is $\lambda v_d(E)/v_g(E)$, where $v_g(E)$ is the (instantaneous) group velocity. This is because the distance drifted downfield between two collisions is $v_d(E) \times \tau = \lambda v_d / v_g$. For length scales in excess of $\lambda v_d / v_g$, the momentum $\hbar\mathbf{k}$ shows uncorrelated fluctuations around a well-defined average value ($m^* \mathbf{v}_s$ in the case of constant effective mass). For the lucky-drift concept to be meaningful,[6] the two characteristic length scales λ and λ_E should obey the relation $\lambda \ll \lambda_E$. In terms of correlation lengths, this says that the particle averages its momentum (i.e., is drifting) over a much shorter scale than it averages its energy.

There is a quantity that has not been mentioned so far, which is the energy correlation time. In the Appendix it is shown that the energy autocorrelation *in space* varies exponentially with x if λ_E is taken to be independent of energy. Similarly the momentum autocorrelation function varies exponentially in time with time constant $\tau(E)$, because the relaxation time $\tau(E)$ is solely determined by an isotropic matrix element (deformation-potential coupling) and the density $N(E)$ of available states at the energy E (with the final energy nearly equal to the initial one, as $E \gg \hbar\omega$). In the case of energy, the relevant relaxation time $\tau_E(E)$ depends on energy, leading to a nonexponential autocorrelation function. The energy correlation time

$$\tau_c = \frac{\int_0^{+\infty} \langle [E(t) - E_{av}][E(t+t') - E_{av}] \rangle dt'}{\langle (E - E_{av})^2 \rangle} \tag{26}$$

cannot be determined in general. If we suppose that E differs little from E_{av} in the course of time, a small-signal expansion gives $\tau_c = (2/3)\tau_E(E_{av})$. In the large-signal case, we shall take $\sim\tau_E(E_{av})$ as an all-purpose estimate of the energy correlation time. This is reasonable unless $\tau_E(E)$ is a strong function of energy, such as occurs around an intervalley separation which usually results in a sudden increase in the density of states.

The average drift velocity expresses the average distance traveled downfield per unit time. The lucky-drift model deals with a local, *energy-dependent* drift velocity $v_d(E) = qF\tau(E)/m^*$, which is determined by the perfectly randomizing nature of the momentum-relaxing collisions, just as in Drude's model of conductivity. The *average* drift velocity at saturation v_s is taken to be $v_d(E_{av})$. The question is now reinvestigated in light of our new statistical tools.

The vector average drift velocity

$$\mathbf{v}_s = (1/t) \int_0^t \mathbf{v}_g(t') dt' \tag{27}$$

(at large t) may also be written

$$v_s = \int_0^{+\infty} v_d(E)(-dP/dE)dE \ . \tag{28}$$

Eq. (28) is derived from (27) by first averaging $\mathbf{v}_g(t)$ over a time $\tau[E(t)] \ll \tau_E(E)$, spent at constant E, which gives $\mathbf{v}_d(E)$ (directed along $\mathbf{F}$). Then we replace the fraction of time the particle has spent at an energy E by $(-dP/dE)dE$. The use of $v_s = \langle v_d \rangle$ makes sense for distances of l_c or more, over which the energy distribution has been virtually explored. The value obtained in this way exceeds $v_d(E_{\rm av})$ by a factor $\sqrt{\pi}$ in the parabolic model, yet the simple estimate $v_s = v_d(E_{\rm av})$ compares favorably with numerical simulations.[12] In fact $v_d(E)$ such as given by the original lucky-drift model is unphysical at low energies, since it exceeds the group velocity for $E < qF\lambda/2$. This arises because $1/\tau$ varies as $N(E) \sim E^{1/2}$, leading to infinite collision times $\tau(E)$ as $E \to 0$. (Near $E = 0$, other scattering mechanisms, not accounted for in the lucky-drift model, set an upper bound to the scattering time and keep v_d below v_g.) As $n(E)$ takes appreciable values for $E \approx qF\lambda$ (Fig. 1), the contribution of infinite v_d's near $E = 0$ overestimates $\langle v_d \rangle$. Therefore we shall retain $v_s = v_d(E_{\rm av})$. Then $\tau_E(E_{\rm av})$ appears as the time needed to drift over a correlation length λ_E, consistent with our using it as the energy correlation time.

We now come to diffusion. When a sheet of carriers leaves the plane $x = 0$, the average drift velocity describes the movement of the centroid of this bunch of carriers along the field. They also diffuse because of the concentration gradient. The diffusion coefficient D is half the mean-square spreading of the pulse of charge carriers in space, after a unit time has elapsed. This leads to the well-known expression of the diffusion coefficient in terms of the velocity autocorrelation function:

$$D = \int_0^{+\infty} \langle [\mathbf{v}_g(t+t') - \mathbf{v}_s][\mathbf{v}_g(t) - \mathbf{v}_s] \rangle dt' \ . \tag{29}$$

The instantaneous velocity will be written down as $\mathbf{v}_g(t) = \mathbf{v}_d[E(t)] + \mathbf{u}(t)$, where $\mathbf{u}(t)$ randomly fluctuates around zero on a scale $\tau[E(t)]$, whereas $\mathbf{v}_d[E(t)]$ fluctuates around $\mathbf{v}_s$ on a scale $\tau_E[E(t)]$. The integrand of (29) may be expanded into

$$\begin{aligned} &\langle \{\mathbf{v}_d[E(t+t')] - \mathbf{v}_s\}\{\mathbf{v}_d[E(t)] - \mathbf{v}_s\} \\ &\quad + \mathbf{u}(t+t')\mathbf{u}(t) + \mathbf{v}_d[E(t+t')]\mathbf{u}(t) \\ &\quad + \mathbf{u}(t+t')\mathbf{v}_d[E(t)] \rangle \ . \end{aligned} \tag{30}$$

In (30) the last two terms average to zero, because $\mathbf{u}$ rapidly fluctuates while $\mathbf{v}_d$ remains nearly constant. Hence

$$D = D_g + D_d \ , \tag{31a}$$

where

$$D_g = \int_0^{+\infty} \langle \mathbf{u}(t+t')\mathbf{u}(t) \rangle dt' \tag{31b}$$

is the diffusion coefficient associated with the fluctuations of the instantaneous velocity $\mathbf{v}_g$ around the local drift velocity [over a scale $\tau(E)$], and

$$D_d = \int_0^{+\infty} \langle \{v_d[E(t+t')] - v_s\}\{v_d[E(t)] - v_s\} \rangle dt' \tag{31c}$$

is the diffusion coefficient associated with the fluctuations of the local drift velocity $v_d(E)$ around the average drift velocity, which occur over a typical time scale $\tau_E(E)$. The general result (31a) is the mere consequence of decoupled time behaviors for momentum and energy due to $\tau \ll \tau_E$. Another general result is that D_g and D_d have the same order of magnitude. To see it we first transform D_g:

$$D_g = \langle u(E)^2 \tau(E) \rangle = \int_0^{+\infty} u^2(E)\tau(E)n(E)dE \ . \tag{32}$$

Approximating $u^2(E)$ by $v_g^2(E)$ [since $v_d(E) \ll v_g(E)$], and taking the spherical parabolic estimate $v_g^2(E) = 2E/m^*$, we get:

$$D_g \simeq 2E_{\rm av}\tau(E_{\rm av})/m^* \ . \tag{33}$$

In (33) we have further assumed that $n(E)$ was sufficiently peaked around $E_{\rm av}$. Equation (33) may be readily checked in the parabolic case. The parabolic energy distribution Eq. (14) yields $D_g = 2\sqrt{\pi}E_{\rm av}\tau(E_{\rm av})/m^*$ in spite of $n(E)$ not being peaked at $E_{\rm av}$ (Fig. 1). What actually matters is not the "peakiness" of the distribution, but the presence of a single characteristic energy, here $E_{\rm av}$. We now transform D_d along similar lines:

$$D_d = \langle [v_d(E) - v_s]^2 \rangle \tau_E(E_{\rm av}) \simeq v_s^2 \tau_E(E_{\rm av}) \ . \tag{34}$$

Owing to the unphysical behavior of $v_d(E)$ near $E = 0$ already outlined, in (34) we simply put v_s^2 as the variance in drift velocity [this is consistent with a small-signal expansion of $v_d(E)$ around $v_d(E_{\rm av})$, which in the parabolic case yields a variance $v_s^2/4$]. Then the expressions of v_s and τ_E lead to $D_g \sim D_d$. To finish with, D may be written as follows:

$$D \sim E_{\rm av}\langle v_d \rangle / qF \ . \tag{35}$$

Equation (35) appears as a generalization of Einstein's relation between mobility μ and diffusion D at low field ($\langle v_d \rangle = \mu F$ and $E_{\rm av} \sim kT$ in the Ohmic, thermalized regime). At high field where $\langle v_d \rangle$ saturates, the diffusion coefficient is expected to scale like $E_{\rm av}/qF$ [Eq. (35)] or $\tau_E(E_{\rm av})$ [Eq. (34)]. As a matter of fact, the experimental $D(F)$ drops at high field,[20] but the intervalley transition gives rise to a peak in $D(F)$ known as straggle diffusion, expressing the fact that the average drift velocities in the low- and high-energy valleys are fairly different.[21] When $E_{\rm av}$ coincides with the intervalley separation E_i in a direct-gap semiconductor, the times τ and τ_E are very strong functions of E owing to the sudden increase in $N(E)$. The hypothesis of a single characteristic time allowing scaling shortcuts in the calculation of D_g and D_d is impracticable, but expressions (33) and (34) for D_g and D_d behave correctly in that a sharp drop in the diffusion coefficients after intervalley transfer is predicted owing to the drop in τ and τ_E, but the peak in $D(F)$ is not reproduced. Nor was reproduced the Ohmic-to-saturated transition in $\langle v_d \rangle$, meaning that lucky drift describes

only the high-field behavior. The use of one characteristic length or time scale will generally not yield good results in the presence of significant intervalley scattering. If statistical averages $\langle A \rangle$ are to be calculated, the use of the full distribution function in Eq. (11) is mandatory. Statistical features specific to the existence of several valleys are tackled in the following subsection.

E. Generalized lucky-drift model

Practical applications[13–16] of the lucky-drift model so far consider the simple case of spherical parabolic bands. It is the version recalled in Sec. II A, which is completely analytical. It predicts that 63% of the carriers can be found at $E < E_{\rm av}$, and that the high-energy tail of the distribution varies as $\exp(-E/E_{\rm av})$, with $E_{\rm av} \sim F^2$. In some instances this poorly reflects the true, or presumed, hot-electron behavior. Simulations in direct-gap materials such as GaAs or ZnS show that the scattering rate steeply increases when satellite valleys appear, due to an enhanced density of available final states. Then the rate of increase of the average hot-electron energy exhibits a sudden drop, so that the smooth relation $E_{\rm av} \sim F^2$ does not make sense any more when $E_{\rm av}$ crosses the intervalley separation energy E_i. If the basis of the lucky-drift concept is sound, such discrepancies are to be ascribed to the use of parabolic-band dispersion relations, even though the mean free path implicitly accounts for a density of conduction-band states largely exceeding that associated with a parabolic band with zero-energy effective mass. Lucky-drift theory in principle is not restricted to parabolic bands. The simplifying features afforded by parabolic bands are: (i) the constancy of $\lambda = v_g(E)\tau(E)$ and $\lambda_E = v_d(E)\tau_E(E)$ with respect to energy for deformation-potential interaction; (ii) a constant effective mass m^*, allowing immediate writing of $v_d(E)$. Actual bands deviate from parabolicity in two ways, that we could name smooth and unsmooth. By smooth we mean that not far from valley minima, the dispersion relation is smoothly altered into[7]

$$\hbar^2\mathbf{k}^2/2m^* = E(1+aE) \tag{36}$$

where a is a nonparabolicity parameter (for simplicity we consider the isotropic case). The consequences are the following: (i) $v_g(E) = (1/\hbar)(dE/dk)$ is less than the parabolic value $(2E/m^*)^{1/2}$; (ii) $m^*(E)$, defined as the "optical" effective mass, increases with respect to m^*, the effective mass at zero energy; and (iii) the density of states $N(E)$ is enhanced together with the collision rate $1/\tau(E)$. As a result of (i) and (iii) the mean free path $\lambda(E)$ decreases at high energies. From (ii) and (iii) the energy relaxation length

$$\lambda_E(E) = qF[\tau(E)]^2 E/[m^*(E)\hbar\omega/(2n+1)] \tag{37}$$

decreases at high energies, too. Ridley[6] worked out a simple model of smooth nonparabolicity, in which $\hbar^2\mathbf{k}^2/2m^* \sim E^{5/4}$ or equivalently $m^*(E) \sim E^{1/4}$ (valid for not too low E's). He found a smooth, nonparabolic average-energy-field dependence, $E_{\rm av} \sim F$, and concluded that a constant effective mean free path, depending on the energy range of interest, could be used safely.

The second, unsmooth deviation from parabolicity corresponds to the case in which the surface in the Brillouin zone belonging to a single energy is not, even approximately, a sphere or an ellipsoid, but a complex surface of several sheets. This is usually associated with the appearance of satellite valleys at high enough energies (the intervalley energy $E_i = 0.35$ eV in GaAs, 1.45 eV in ZnS). McKenzie and Burt[22] applied the lucky-drift theory to a multivalley model semiconductor, and found fairly good agreement with the Monte Carlo predictions, but not so uniformly good as in the parabolic monovalley case.[12] This was tentatively attributed to a discrepancy between the "true" (i.e., Monte Carlo–simulated) and the lucky-drift trajectories, and the present work supports their conclusion. In the multivalley case band-structure-related quantities such as $\mathbf{v}_g$ and m^* do not depend on E only, but also on the electron position $\mathbf{k}$ in the Brillouin zone. The scattering rate $1/\tau$ is also a function of $\mathbf{k}$, and $1/\tau$ as a function of E means an average over a constant-energy surface in the phase space. Specifically we mean:

$$1/\tau(E) = \frac{\sum_n \int d\mathbf{k}\, \tau^{-1}(\mathbf{k},n)\delta[E_n(\mathbf{k}) - E]}{\sum_n \int d\mathbf{k}\, \delta[E_n(\mathbf{k}) - E]}, \tag{38}$$

where n is a sheet or valley index. This averaging in $\mathbf{k}$ space favors the valleys of higher density of states, where the electrons spend a larger time. Then the energy relaxation rate $1/\tau_E$ is defined as a function of E through Eq. (1); a single phonon angular frequency ω is used, which is, for example, an average of optical and zone-edge acoustic phonon frequencies.

A definition of *spatial* rates $1/\lambda$ and $1/\lambda_E$, which are central to the lucky-drift model, needs some care. Strictly speaking, both depend on the wave vector $\mathbf{k}$, and lucky drift is still a valid concept provided that, for all $\mathbf{k}$ at a given E, $\lambda_E \gg \lambda$. Then momentum relaxes over much smaller space-time scales than does energy. Since the electron-phonon interaction connects Bloch states of nearly equal energies ($\hbar\omega \ll E$), it is possible to average $1/\lambda$ over a constant-energy surface in phase space and view the ensuing λ as the mean free path, or momentum relaxation length, for an electron of energy E. Similarly, a constant-energy average of $\lambda_E^{-1}(\mathbf{k}) = [v_d(\mathbf{k})\tau_E(\mathbf{k})]^{-1}$ may be performed, so that λ^{-1} and λ_E^{-1} are now functions of energy. Some points or small regions of the phase space may exhibit singular behavior caused by a vanishing group or drift velocity. This would require a specific, material-dependent examination, for which a numerical approach is better suited, and is contrary to the aim of the paper, which is devoted to the understanding of universal trends, in the spirit of Ridley's lucky-drift approach. Thus in the following we shall simply suppose that both the mean free path and the energy relaxation length can be meaningfully defined as functions of energy, and test the behavior of the lucky-drift model in the case of energy-dependent λ and λ_E. This we shall call the "generalized lucky-drift model," and it is to the investigation of its statistics that we now turn.

We first establish the general expression for the energy

distribution function and apply it to a simplified example borrowed from a Monte Carlo simulation[23] using a full band structure. The probability for an electron to reach energy E in a field F is a generalization of Eq. (4):

$$P(E)=\exp\left[-\int_0^z dz'/\lambda(z')\right] + \int_0^z \exp\left[-\int_0^{z'} dz''/\lambda(z'')\right][dz'/\lambda(z')] \times\exp\left[-\int_{z'}^z dz''/\lambda_E(z'')\right], \quad (39)$$

where we have used the lucky-drift variable $z=E/qF$, and the rates $\lambda^{-1}(E)$ and $\lambda_E^{-1}(E)$ depend on energy, in contrast to the original Eq. (5). The first term is the probability of a ballistic flight up to z, while the second one sums all lucky drifts starting at z' between 0 and z; $\lambda(z)$ [$\lambda_E(z)$] stands for $\lambda(E)$ [$\lambda_E(E)$] wherein $z=E/qF$. It is useful to notice that $P(z)$ satisfies a simple differential equation:

$$\frac{dP}{dz}=-\frac{1}{\lambda_E(z)}[P(z)-P_{\rm LB}(z)], \quad P(0)=1, \quad (40)$$

where

$$P_{\rm LB}(z)=\exp\left[-\int_0^z dz'/\lambda(z')\right] \quad (41)$$

is the probability of lucky-ballistically reaching z.

Since the dominant term in (39) is expected to be the probability of lucky drifting to E, viz.,

$$P_{\rm LD}(E)=\exp\left[-\int_0^z dz'/\lambda_E(z')\right], \quad (42)$$

we rewrite $P(E)$ differently, using an integration by parts:

$$P(E)=\exp\left[-\int_0^z dz'/\lambda_E(z')\right] + \int_0^z \exp\left[-\int_0^{z'} dz''/\lambda(z'')\right][dz'/\lambda_E(z')] \times\exp\left[-\int_{z'}^z dz''/\lambda_E(z'')\right]. \quad (43)$$

Since $\lambda_E \gg \lambda$, the second term in the right-hand side of (43) should be negligible, except at low, finite E. If it is dropped we find that $P(E)\simeq P_{\rm LD}(E)$.

The energy distribution of the new model, $n(E)=-dP/dE$, may be straightforwardly derived from the differential equation (40). Taking $P(E)\simeq P_{\rm LD}(E)$, we may retain as a good approximation:

$$-dP/dE\simeq[qF\lambda_E(E)]^{-1}[P_{\rm LD}(E)-P_{\rm LB}(E)]. \quad (44)$$

This generalized expression of the electron energy distribution $n(E)$ vanishes for $E\to 0$ or $+\infty$; the high-energy tail is controlled by the asymptotic behavior of $\lambda_E(E)$, in the spirit of the lucky-drift theory.

In order to check our generalized model in a concrete case, we turn to a numerical simulation of transport in ZnS which made use of a realistic band structure.[23] Zinc sulfide is a wide ($E_g=3.7$ eV), direct bandgap semiconductor where the intervalley separation in the empirical-pseudopotential band-structure model is $E_i=1.45$ eV (almost the same for Γ-X and Γ-L). There is a sharp rise in the density of conduction-band states as E_i is crossed, and associated therewith a fourfold increase in the collision rate over less than 0.1 eV. The electron distribution in energy space (Fig. 2) is found to be localized in the upper neighborhood of E_i for F ranging between 0.5 and 1 MV/cm, with very few carriers beyond 2.1 eV (<1% according to Ref. 23). From Fig. 2 we compute $E_{\rm av}=1.50$ and 1.71 eV at $F=0.5$ and 1 MV/cm. The original lucky-drift model predicts that $E_{\rm av}\sim F^2$ should increase by a factor of 4 over that field range, and thus poorly describes the situation. Can we reproduce the "true" (i.e., Monte Carlo–simulated) behavior in the generalized lucky-drift framework? Disregarding smooth nonparabolicity effects, we take the spatial collision rate to be a steplike function of the simplest kind:

$$\lambda^{-1}(E)=\lambda_1^{-1}+(\lambda_2^{-1}-\lambda_1^{-1})\frac{\exp[(E-E_i)/\Delta_i]}{1+\exp[(E-E_i)/\Delta_i]}, \quad (45)$$

where 1 stands for low energy ($E<E_i$), and 2 for high energy ($E>E_i$). The function has a Fermi-Dirac-like variation, changing from λ_1 to λ_2 around E_i within an interval $\sim\Delta_i$ taken to be 0.07 eV. The values of λ_1 and λ_2 are computed through $\lambda(E)=v_g(E)\tau(E)$ at $E=1$ and 2 eV. The scattering times $\tau_1=10^{-14}$ s and $\tau_2=0.2\times10^{-14}$ s are from the simulation (Fig. 4 of Ref. 23). Computation of the group velocity $v_g(E)$ accounting for $m^*=0.3m_0$ and a nonparabolicity parameter $a=0.69$ eV^{-1} yields $v_1=0.58\times10^8$ cm/s and $v_2=0.62\times10^8$ cm/s. Therefore $\lambda_1=58$ Å and $\lambda_2=12.3$ Å. The parameters are listed in Table I. As for $\lambda_E^{-1}(E)$, it is deduced from $\lambda(E)$ through Eq. (3), where $\frac{1}{2}$ is the parabolic-band value of $E/[m^*(E)v_g(E)^2]$. If the $E(\mathbf{k})$ relation (36) is used, we

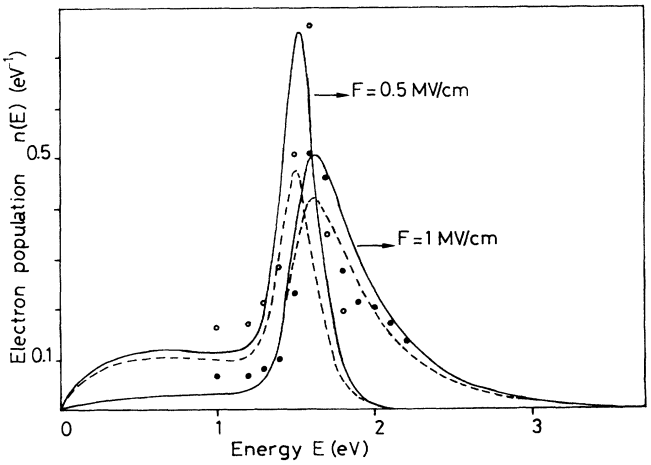

FIG. 2. Electron population $n(E)=N(E)f(E)$ in ZnS at 300 K, according to a Monte Carlo simulation in a realistic band structure (after Figs. 2 and 8 of Ref. 23): open circles, $F=0.5$ MV/cm; full circles, $F=1$ MV/cm. Normalized electron population $n(E)$ in ZnS at 300 K, according to the generalized lucky-drift model with energy-dependent, steplike $\lambda(E)$ (parameters in Table I): Solid line, exact $n(E)$ [Eq. (40)]; dashed line, approximation Eq. (44).

TABLE I. Parameters for the generalized lucky-drift model (ZnS).

Phonon energy $\hbar\omega$ (meV)	Effective mass m^*/m_0	Nonparabolicity a (eV^{-1})	Intervalley separation E_i (eV)	Δ_i (eV)	Low-energy free path λ_1 at 300 K (Å)	High-energy free path λ_2 at 300 K (Å)
42	0.3	0.69	1.45	0.07	58	12.3

find that $\frac{1}{2}$ should be replaced by $(1+2aE)/[2(1+aE)]\sim 0.75$ in the 1–2-eV range. This is taken into account in the computation of $\lambda_E^{-1}(E)$. The electron population $n(E)$, both exact [Eq. (40)] and approximate [Eq. (44)], has been displayed in Fig. 2 for the fields $F=0.5$ and 1 MV/cm. In this example, the difference between $P(E)$ and $P_{\rm LD}(E)$ is noticeable owing to the smallness of the high-energy free path, making the condition $\lambda/\lambda_E \ll 1$ moderately satisfied. The area under the exact $n(E)$ curve [solid line, Eq. (40)] is $P(0)=1$; the area is less than unity in the case of the approximate $n(E)$ curve [dashed line, Eq. (44)]. The agreement with the Monte Carlo results in Fig. 2 is striking. Just as in previous comparisons,[12,22] we do not make use of any disposable parameter. It is seen that over that field range most carriers remain in the upper neighborhood of the intervalley energy, with a high-energy tail growing with field. The effect of increasing the field hardly modifies the peak of $n(E)$ slightly above E_i, but enhances the rms width of the distribution, thereby pushing up the average energy. Of course the long-lasting tail is also the result of a constant energy relaxation length at high energy, so that the present calculation based upon (45) is not expected to represent accurately the Monte Carlo–simulated results for $E_{\rm av}>2$ eV (not available in Ref. 23). At very high energy, $1/\tau$ is bounded ($\leq 7\times 10^{14}$ s^{-1}), so that the long-lasting tails do not seem unphysical. Other conduction bands (not calculated in Ref. 23) will eventually come into play and decrease the energy relaxation length. Another possible drop in $\lambda_E=v_d(E)\tau_E(E)$ is expected if umklapp electron-phonon processes giving rise to backward scattering[24] decrease the high-energy drift velocity $v_d(E)$.

Since the $n(E)$ from the Monte Carlo and lucky-drift models are very close, so should be the average energies. The $E_{\rm av}$'s at $F=1$ MV/cm are remarkably close (Monte Carlo: 1.71, lucky drift: 1.79 eV). Our Monte Carlo estimation $E_{\rm av}=1.50$ eV at $F=0.5$ MV/cm suffers from the absence of reliable $n(E)$ at $E<1$ eV. If the lucky-drift average is computed for $E\geq 1$ eV to allow a safer comparison, we find 1.49 eV. The agreement is impressive given the simplicity of the analytical model. Note that at low energy, polar scattering prevails in ZnS, so that no great accuracy is expected from the lucky-drift description.

Figure 3 shows the average energy $E_{\rm av}$ and the demarcation energy $E_{1/2}$ [for which $P(E_{1/2})=\frac{1}{2}$] as functions of field F in the generalized lucky-drift model. The two energies are not very different. The average-energy-field dependence is noticeably sublinear, and tracks that expected from numerical simulations[8,23] [Fig. 11 of Ref. 8 gives $E_{\rm av}(F)$ in GaAs around $E_i\simeq 0.35$ eV]. Figure 3 also shows $E_{\rm av}/qF$ together with $\lambda_E(E_{\rm av})$. The difference is important due to the large range of values taken by $\lambda_E(E)$ in such a multivalley model. Which is closest to the correlation length? Once most electrons have overtaken E_i, $\lambda_E(E)$ is almost constant over the width of the energy distribution, and the Appendix shows that $\lambda_E(E_{\rm av})$ is the energy correlation length. At low fields such that most electrons lie within the central valley, $\lambda_E(E_{\rm av})\sim\lambda_1^2 F$, and $\lambda_E(E_{\rm av})\sim\lambda_2^2 F$ once $E_{\rm av}$ exceeds E_i. The use of one correlation length $\lambda_E(E_{\rm av})$ is adequate for $F\gtrsim 1$ MV/cm, see Fig. 2. At $F\approx 0.5$ MV/cm, corresponding to $E_{\rm av}$ or $E_{1/2}\approx E_i$, the consideration of one correlation length is inappropriate, and the autocorrelation function for $E(x)$ is expected to be strongly nonexponential.

From this example it follows that the lucky-drift statistical device, namely, the calculation of the possible energies from "unphysical" flights starting from zero energy, reminiscent of the Shockley lucky-electron concept, leads to an essentially correct energy distribution if realistic relaxation lengths are used. In previous subsections, we have emphasized the artificial character of the lucky-drift trajectories, which lead to correct statistics insofar as energy is concerned. In fact two cases should be distinguished. The consideration of those flights starting from zero energy is fully relevant in the study of *transient* transport, for instance, in the nonlocal model described in Ref. 14 (in which, however, the expression for the impact ionization rate should be corrected according to the remarks of Sec. III). In the case of thermal carriers injected at a heterojunction they can yield the fraction of ballistic electrons. Concerning *bulk*, steady-state transport, however, the notion of ballistic carriers is not adequate, since after a sufficient time or length, all carriers

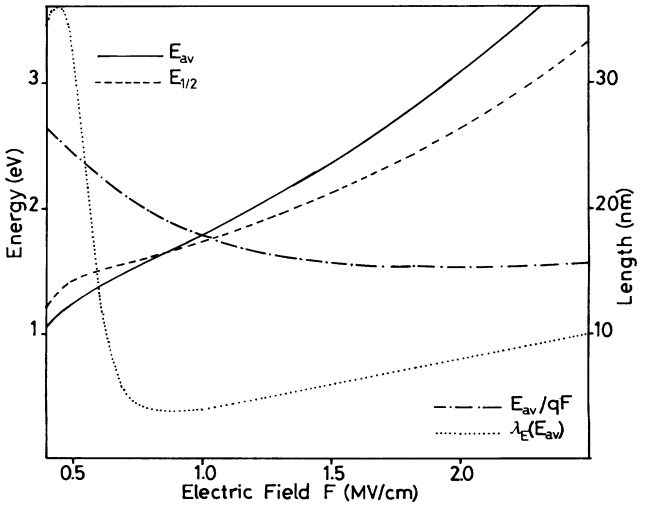

FIG. 3. Average energy $E_{\rm av}$, demarcation energy $E_{1/2}$, and energy correlation lengths $E_{\rm av}/qF$ and $\lambda_E(E_{\rm av})$ as functions of field F in ZnS at 300 K, according to the generalized lucky-drift model (parameters of Table I).

eventually enter the drift regime. Shichijo and Hess[8] have shown that "lucky" electrons actually start from the average energy. They are lucky in the sense that they escape significant energy relaxation while gaining energy from the field. Because this is reflected in the derivation of $P(E)$ based upon an energy-dependent λ_E, correct statistics for $n(E)$ ensues.

III. IMPACT EXCITATION

The purpose of this section is twofold. First, we revise an earlier calculation[15] of the hot-electron-impact excitation rate α_e of a deep impurity. That impact process is the basis of the operation of so-called high-field electroluminescence display devices, where the impacted impurity returns to its ground state by emitting visible light. The previous calculation rests on the use of the lucky-drift trajectories, similar to the derivation[17] of the band-to-band impact-ionization rate α_n in the case of a soft threshold. The application of our new statistical rules will result in a different expression for α_e, which will be compared with the original one and with experimental data.[15] Second, in addition to practical reasons there are also fundamental reasons to undertake this task. We wish to emphasize that impact excitation can, better than impact ionization, serve as a test of transport theories. Because impact excitation is simply the inelastic collision of an energetic carrier with an impurity, it is a one-body process which is easier to deal with than carrier-induced hole-electron pair production, a three-body process. For instance only recently[1,17] was it realized that the ionization probability is rather small jut above the energy-momentum threshold for pair production, so that the rate α_n is not straightforwardly related to the fraction of carriers reaching the threshold energy. In spite of Kane's early theoretical calculation[25] in Si, it was a surprise in 1981 to find effective threshold energies[26] for impact ionization largely exceeding the E_g or $\frac{3}{2}E_g$ values. A straightforward consequence is that hole-electron pair creation negligibly affects the hot-electron distribution function, see Fig. 7 of Ref. 27. Furthermore, the very values for the energy-momentum threshold such as predicted by Anderson and Crowell[28] have recently been shown[29] to be in error. More importantly, owing to the complexities of the band structure there may be several thresholds in $\mathbf{k}$ space, of unequal softness, as well as antithresholds,[1,30] making the interpretation of the observed α_n awkward. In contrast, the inelastic collision of a high-energy electron on an impurity is characterized by only one threshold (per excited level of the center), which is readily obtained from the excitation spectrum of the atom. Hence the ensuing electroluminescence just samples the high-energy tail of the distribution, and it is argued in Sec. III D that $P(E)$ could be directly measured. A third advantage afforded by measuring α_e's instead of α_n's is the constancy of current in the former case. When hole-electron pairs are created, the electron current is not homogeneous along the sample thickness, and the newly crated electrons do not belong to the steady-state distribution $n(E)$ under investigation. Only after some drift downfield are they "thermalized." Additionally, a hole current traverses the material, possibly giving rise to undesired extra effects. Other drawbacks inherent in the use of α_n's to probe the hot-electron energy distribution have been pointed out by Capasso.[1] Impact excitation of an impurity and impact ionization of the lattice have one common drawback, which is the incomplete knowledge of the cross section of either process as a function of energy above threshold. Yet the theory of the one-body process is easier to work out than that of the three-body process.

A. Impact excitation rate

By E_e we denote the energy threshold for impact excitation, and by $\sigma(\mathbf{k})$ the total cross section for an incident electron of wave vector $\mathbf{k}$. Strong orientational dependence of σ with respect to the crystal axes has been found in a theoretical calculation[31] based on the Born approximation (i.e., Fermi's Golden rule). Note that this orientational dependence of $\sigma(\mathbf{k})$ has nothing to do with that of the impact-ionization rate α_n, which in the early works was attributed[1] to an anisotropy in transport *prior* to the impact process.

The rate of impact excitation α_e is defined as the expected number of excitations per unit length per charge carrier. Just as its analogue α_n, it is also[26] the number of carriers impacted per unit time per unit volume, normalized to the incident flux (carrier current per unit area). The second definition straightforwardly yields a mathematical expression for α_e. Taking one incident electron per unit area, the incident flux is $\langle v_d \rangle = v_s$. When the electron's energy $E(\mathbf{k})$ is in excess of the threshold E_e, its probability per unit time to collide with a center is $\sigma(\mathbf{k})v_g(\mathbf{k})$, to be multiplied by the number of centers per unit volume n. Since momentum is relaxed more rapidly than energy, we average this in $\mathbf{k}$ space over a constant-energy surface $E(\mathbf{k})=E$, and define an *effective isotropic* cross section $\sigma(E)$ and group velocity $v_g(E)$ as

$$\sigma(E)=\langle \sigma(\mathbf{k})v_g(\mathbf{k}) \rangle / \langle v_g(\mathbf{k}) \rangle \ , \tag{46a}$$

$$v_g(E)=\langle v_g(\mathbf{k}) \rangle \ . \tag{46b}$$

The collision probability per unit time per unit volume is $n\sigma(E)v_g(E)$, the ensemble average of which is [Eq. (11) of Sec. II]

$$\int_{E_e}^{+\infty} n\sigma(E)v_g(E)(-dP/dE)dE \ ,$$

so that

$$\alpha_e = \frac{1}{v_s} \int_{E_e}^{+\infty} n\sigma(E)v_g(E)(-dP/dE)dE \ . \tag{47}$$

The expression obtained previously,[15] based on the picture of lucky-drift trajectories, is

$$\alpha_e' = \int_{E_e}^{+\infty} n\sigma(E)\frac{v_g(E)}{v_d(E)}P(E)dE/E \ . \tag{48}$$

The expressions differ in two ways (not to mention the orientation averaging). The first difference lies in the drift velocity used. In Eq. (48) the values of $v_d(E)$ which

matter are just above the energetic threshold E_e, while in Eq. (47) v_s is deemed to be $v_d(E_{av})$. At low fields where $E_e \gg E_{av}$, the drift velocity used in Eq. (48) will tend to overestimate the impact rate per unit length. The second difference lies in the weighting factor. In $\alpha'_e n(E)$ is replaced by $P(E)/E$. If, as is the usual case, E_e is high enough that it cannot be reached ballistically, then $n(E)=P(E)/[qF\lambda_E(E_e)]$ just above E_e. So the integrand of α'_e contains E_e as a denominator instead of $qF\lambda_E(E_e)$. At low fields the effect of incorrect statistics in α'_e will tend to be an underestimate of the impact rate. Therefore the two differences between α_e and α'_e might partly offset each other. But more importantly, the field dependence of the two expressions [in $P(E)$ and $v_d(E)$] is different. A quantitative comparison between α_e and α'_e can be found in Sec. III C, where both deviations will be found.

B. Impact statistics

In the presence of excitable centers, an electron moving over a distance d along the field suffers $\alpha_e d$ inelastic collisions. If, as is the usual case (see Sec. III C), the average distance between two excitation events α_e^{-1} is large compared to the correlation length, electron transport will not be affected by impact excitation, and the statistics of impacts will obey simple laws similar to those outlined in Sec. II C. The collisions occur independently, with a well-determined average number $\alpha_e d$. Independence does not hold on very short spatial scales, since just after an inelastic collision, an electron is unlikely to be hot enough to excite a center. But if the length over which the impacted electron returns to the steady state, which is of the order of the relaxation or correlation length, is shorter than the average distance between collision, α_e^{-1}, the perturbation will be insignificant, and the electron will rapidly lose the memory of the previous collision. Collisions occurring at random with a well-defined probability per unit length obey Poisson statistics. The average number of impacts is $\alpha_e d$, the probability that no impact take place is $\exp(-\alpha_e d)$, and the probability of n impacts is $(\alpha_e d)^n \exp(-\alpha_e d)/n!$ The variance in the number of impacts, which is related to the noise, is $\alpha_e d$. In the case of a small impact-excitation rate ($\alpha_e d < 1$), a large noise is expected. The notions developed in this subsection may be applied, *mutatis mutandis,* to impact-ionization statistics; this will modify the noise-figure calculations derived from the lucky-drift trajectories.[16]

C. Hard-threshold case

The probability of band-to-band impact ionization does not vary from zero to unity as the energy-momentum threshold is crossed: the threshold is "soft."[1,17,18,32] In Keldysh's theory,[33] which is based on the golden rule, the probability for pair production grows as the square of the excess energy; depending on the $E(\mathbf{k})$ relationship, in some parts of the Brillouin zone it may exhibit a different functional form.[34] Similarly, in the case of an impact-excitable impurity, the cross section $\sigma(E)$ smoothly increases[31] from zero above the threshold energy E_e. Here again it is simpler to deal with a hard-threshold excitation process, by which it is meant that $\sigma(E)$ is a steplike function equal to σ_0 if $E > E_e$. The consideration of a finite impact-excitation cross section right from threshold is naturally a simplification, but it is more easy to justify than its impact-ionization counterpart. If first-order perturbation theory is used (in collision theory it is named the Born approximation), $\sigma(E)$ is proportional to the density of final states: Since the final energy $E - E_e$ lies near the bottom of the conduction band, $N(E-E_e)$ will assume a parabolic form $\sim(E-E_e)^{1/2}$, that is, it will sharply increase in the vicinity of E_e, in contrast to the form of the impact-ionization cross section $\sim(E-E_i)^2$. Hence in this subsection we particularize the expression for α_e obtained in Sec. III A to the case of a finite impact cross section σ_0 right from threshold. Equation (47) then yields:

$$\alpha_e = n\sigma_0 v_g(E_e)P(E_e)/v_s \ , \tag{49}$$

wherein we have further approximated $v_g(E)$ to a constant above E_e [this is justified in the framework of the Born approximation which gives[35] the *product* $\sigma(E)v_g(E)$ as a squared matrix element times $N(E-E_e)$]. The meaning of (49) is obvious. For a hot electron, the time-independent impact-excitation probability per unit time $n\sigma(E)v_g(E)$ is multiplied by the fraction of time $P(E_e)$ spent above E_e, and v_s converts the time rate into a spatial rate. It is worthy of remark that the previous expression[15] α'_e does not meet that requirement, and thereby is not physical. Equation (49) shows that α_e is a direct indicator of the fraction of electrons overtaking a certain energy, making it an interesting observable for testing high-field transport theories. More specifically, if $\sigma(E)v_g(E)$ varies as $(E-E_e)^{1/2}$ over the energy scale $E_0 = -\{d \ln[P(E)]/dE\}^{-1}$ at threshold, then in Eq. (49) one simply has to replace $\sigma_0 v_g(E_e)$ by $\frac{1}{2}\sqrt{\pi}(\sigma v_g)(E_e+E_0)$. Taking $P(E)$ in ZnS at 300 K from our example of Sec. II E, with $E_e = 2.24$ eV, and $\sigma(E)v_g(E) = 10^{-9}$ cm^3 s^{-1} ($E > E_e$), $n = 5\times10^{18}$ cm^{-3} as reasonable values, we have displayed in Fig. 4 α_e and α'_e/α_e versus electric field. The strong field dependence of α_e just reflects that of $P(E_e)$, and the older expression α'_e, which coincides with α_e for $F = 1.5$ MV/cm and $T = 300$ K, may severely depart from the true value, especially at lower fields.

D. Comparison with experiment

The best-studied[36] impact-excitable impurity is Mn^{2+} in ZnS. It is an isoelectronic substitute of Zn^{2+} which is electrically inactive. The first excited level ($^4T_1$ in crystal-field notation) is at 2.24 eV above the ground state, the next ones (denoted by $^4T_2$ and ^4E) lie at 2.46 and 2.64 eV (excitation energies from Table I of Ref. 36). The observed yellow luminescence is at 2.12 eV (585 nm) due to Stokes shift, and is the basis of a successful solid-state flat-screen technology. We have used low-Mn-doped ZnS layers ($n < 6\times10^{18}$ cm^{-3}) since a high Mn^{2+} concentration ($n \sim 10^{20}$ cm^{-3}) is known to alter the electrical characteristics. The 550-nm-thick layer is

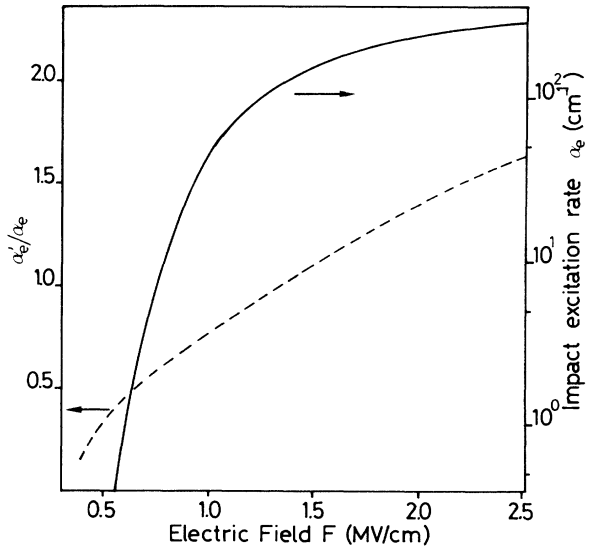

FIG. 4. Impact-excitation rate α_e (this work, revised statistics) in the hard-threshold approximation [$E_e=2.24$ eV, $n\sigma(E)v_g(E)=0.5\times10^{10}$ s^{-1} for $E>E_e$], versus field F at 300 K. The dashed line shows the ratio of α_e' [Eq. (48)] to α_e [Eq. (47) or (49)]. The transport model is that illustrated in Figs. 2 and 3 and refers to ZnS.

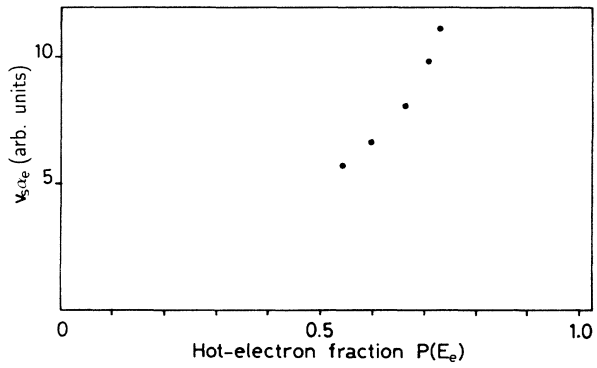

FIG. 5. Test of Eq. (49) for α_e: $[2n(\omega)+1]^{-1/2}L_0\sim v_s\langle\alpha_e\rangle$ has been plotted against the calculated P (2.24 eV) over the investigated temperature range (80–370 K). The transport model is that illustrated in Figs. 2, 3, and 4.

sandwiched between two 330-nm oxide layers, which are perfectly insulating, in order to avoid possible breakdown of ZnS at high field. Upon application of a high enough voltage across the stack, conduction appears in the ZnS film. The field is applied by means of a short (2-μs) voltage pulse, during which F is approximately clamped at 2.0 MV/cm. Approximate clamping in the sulfide arises from the rapid increase of carrier emission rate with field together with the counteracting effect of the field produced by the charge transferred up to the sulfide-oxide boundary. A rise in the peak voltage causes an increase in the charge transferred across the ZnS layer. Correspondingly there is an increase in the number of excited centers, of which the luminescence L_0 (in photons/s) is recorded before they deexcite. L_0 is proportional to the number of excited centers and thus is a measure of α_e. In Fig. 3 of Ref. 15, L_0 was plotted against the transferred charge, with temperature as a parameter. It was seen that (i) L_0 is linear in the transferred charge, reflecting the (approximate) field clamping, and (ii) L_0 decreases at high temperature, consistent with an increased phonon scattering cooling down the hot-electron distribution. According to Eq. (49) $v_s\alpha_e$ should be proportional to $P(E_e)$. That relationship, by which the theoretical $P(E_e)$ may be supported or falsified, may be checked either through the field or the temperature dependence. In the above-described capacitive structures the field cannot be monitored and is approximately clamped, and thus we are forced to rely on the temperature dependence. $v_s\alpha_e$ is measured in arbitrary units through v_sL_0, with $v_s\sim[2n(\omega)+1]^{-1/2}$ [no experimental data for $v_s(T)$ being available]. $P(E_e)$ is computed at $E_e=2.24$ eV from the transport model for ZnS over the range 80–370 K. The comparison is shown in Fig. 5. Contrary to the prediction we do not observe linearity between $v_s\alpha_e$ and $P(E_e)$. This can be ascribed to many reasons, among which only a few will be mentioned. (i) The key parameter controlling the mean free path at high energy is the deformation-potential constant with large-wave-vector phonons, which is not known in ZnS (Ref. 23 merely uses the GaAs value). (ii) The temperature dependence enters through the Bose-Einstein factor $[\exp(\hbar\omega/kT)-1]^{-1}$ in which a single phonon angular frequency ω is assumed. This assumption is good for optical phonons which in ZnS do exhibit a flat dispersion relation[37] ($\hbar\omega=42\pm2$ meV), but questionable for zone-edge acoustic phonons[37] (25 meV) which partake in intervalley transitions. (iii) Indirect evidence exists[38] that the electric field in ZnS layers grown by atomic-layer epitaxy is not uniform, especially at low temperature. This is confirmed by the observation that L_0 depends on the polarity of the applied voltage while the average field is clamped at approximately the same value. The strong field dependence of $P(E_e)$, shown in Fig. 4, makes the comparison unreliable in spite of a qualitatively correct behavior with respect to temperature.

There also exist dc-coupled sputtered ZnS:Mn^{2+} films (metal-insulator-metal structures) which are more prone to breakdown, but where the field is readily monitored through the applied voltage. Then the F dependence of $P(E_e)$ could be tested. But in those samples also the field was not uniform[39] along the layer thickness, owing to unidentified flaws that depended on the process. Correspondingly the light emitted was *sublinear*[39] with respect to the current in spite of an increasing (average) field. It is hoped that another process or material may give a uniform field and thereby allow a safe comparison between impact-excitation yield measurements and theoretical predictions. (The nonlocal transport model,[14] which assumes a nonuniform field profile and predicts negative differential resistance for certain thicknesses, was found not to be obeyed in sputtered ZnS films,[39] suggesting that deep-level ionization does not play a major role in high-field conduction in those films.)

IV. CONCLUSIONS

In this paper we have set up a theoretical dialogue between two descriptions of high-field transport in wide-gap semiconductors. One is analytical and therefore has often been restricted to parabolic bands, whereas the other is a computer simulation allowing inclusion of a realistic band structure. The same physical ingredients, such as deformation-potential electron-phonon interaction, enter both descriptions, which only differ in handling the statistics, and thus should ultimately converge. By bringing them into closer contact, each class of theories can offer a lateral insight into the other one. Starting from the lucky-drift approach, which subsumes previous analytical models, we have compared it with the statistical philosophy of the Monte Carlo simulation. In a first stage, this has provided us with better instructions for use of the lucky-drift model: the artificial character of the so-called lucky-drift trajectories has been highlighted, and they have been replaced by the concept of an energy correlation length of a drifting particle. In a second stage, we have reproduced numerical results obtained in a strongly nonparabolic band structure in the frame of the generalized lucky-drift model, without using adjustable parameters. A more detailed comparison such as performed in Refs. 12 and 22 is obviously desirable, but requires Monte Carlo facilities which are not available to us. The close correspondence between the generalized lucky-drift model and the Monte Carlo approach allows a much simpler understanding of transport statistics than computer simulations, without resorting to oversimple models ignoring the true band structure. In the same way, the correspondence should make the Monte Carlo procedure look less opaque to nonexperts than it has sometimes seemed. Of course, where a detailed or accurate knowledge of transport in a particular material is required, the Monte Carlo method is irreplaceable. But our generalized lucky-drift model affords an overview pointing to the relevant parameters and the chemical trends. In this conclusion we wish to reiterate that the ideal approach lies in the conjugate use of both viewpoints, as was done in the present paper which aimed at a cross fertilization of both descriptions.

Section III has applied the new statistical rules to the calculation of the impact-excitation rate of an impurity. The discrepancy between the present and the former expression is noticeable, and a similar revision should be undertaken regarding impact-ionization rates. It has been argued that the impact-excitation rate of an impurity should be a much better indicator of the fraction of carriers overtaking a certain energy than was the band-to-band impact-ionization rate. The comparison with experiment is straightforward if the electric field is uniform, and should serve as a test of transport theories.

ACKNOWLEDGMENTS

I am indebted to Marc Beale for stimulating discussions about Ref. 39 prior to publication, and to Max Fischetti for his very clear account of the present status of high-field transport simulations. I thank Eric Clément for helpful discussions about statistics.

APPENDIX

The Appendix is devoted to setting up the notion of an energy correlation length of a high-energy drifting carrier, which provides a new look at, and a firmer ground for, the lucky-drift framework. Being of a statistical nature, the notion is also of interest in numerical simulations of transport.

We write first the energy-balance equation

$$\frac{dE}{dt}=qFv_d(E)-\frac{E}{\tau_E(E)} . \tag{A1}$$

The stationary solution ($dE/dt=0$) is obtained for $E^*=qF\lambda_E$. For $E>E^*$, the energy gain from the field is overcome by the loss to the lattice, so that $E\rightarrow E^*$. And if $E<E^*$, more energy is gained by drifting downfield than is lost to the phonons, so that E will increase toward the value achieving balance. Whatever the initial carrier energy at zero time, Eq. (A1) gives one final value, E^*. Equation (A1) is a monoenergetic approach which correctly yields the average energy $E_{\rm av}=qF\lambda_E$, but not the fluctuations around the average. A standard way to introduce the fluctuations is the Langevin approach,[40] in which a random power (averaging to zero) is added to the right-hand side of (A1). This will be done here with the difference that we shall investigate the spatial, instead of temporal, evolution of E, viz.,

$$\frac{dE}{dx}=qF-\frac{E}{\lambda_E}+f(x) . \tag{A2}$$

The x axis is directed downfield, qF is the rate of energy gained per cm, and E/λ_E is the loss. In the original lucky-drift model, λ_E is constant (independent of energy), whence $E^*=E_{\rm av}$. This feature is retained for the moment. As in the Langevin approach, the physical picture is that random kicks, embodied in $f(x)$, cause a tendency for E to spread away from the energy-balancing value E^*, while the damping term E/λ_E tries to bring E back to E^*. $f(x)$ is assumed to satisfy

$$\langle f(x)\rangle=0 , \quad \langle f(x)f(x')\rangle=\Gamma\delta(x-x') , \tag{A3}$$

where $\langle\ \rangle$ means the statistical average over a large ensemble of particles. The condition on the first moment entails that $\langle E\rangle$ satisfies energy balance, and $E_{\rm av}=qF\lambda_E$. The condition on the second moment states that at two different points $x'\neq x$ the random force f is uncorrelated. This is true at large enough spatial scales. The path traveled between two carrier-lattice interactions is λ, the corresponding x drifted downfield is $\lambda v_d(E)/v_g(E)$: below that scale our Langevin description through (A2) breaks down. If δE denotes $E-E^*$, we have

$$\frac{d(\delta E)}{dx}=-\frac{\delta E}{\lambda_E}+f(x) . \tag{A4}$$

The energy autocorrelation function *in space* is $\langle\delta E(x)\delta E(x')\rangle$. From (A4) we obtain

$$\langle \delta E(x)\delta E(x')\rangle = \exp[-(x+x')/\lambda_E]\left\{\langle \delta E(0)^2\rangle + \int_0^x dx_1 \int_0^{x'} dx_2 \exp[(x_1+x_2)/\lambda_E]\langle f(x_1)f(x_2)\rangle\right\} .$$

The first term vanishes far away from the origin $x=0$, and the double integral is computed from (A3). The result is $(x'>x)$,

$$\langle \delta E(x)\delta E(x')\rangle = (\Gamma\lambda_E/2)\exp[-(x'-x)/\lambda_E] . \quad \text{(A5)}$$

The energy autocorrelation function fades away exponentially with distance, and the energy correlation length is just $\lambda_E = E_{\rm av}/qF$. Γ, which measures the strength of the random kicks, is related to the rms deviation from the average energy:

$$\Gamma = (2/\lambda_E)\langle (E-E_{\rm av})^2\rangle . \quad \text{(A6)}$$

Our simple analysis rests on a constant (energy-independent) relaxation length λ_E. In an actual band structure it is more realistic to consider that λ_E at a given F, just like λ, decreases at high energy. If the variation of λ_E is small over the rms width of the energy distribution, a small-signal expansion around the value E^* achieving energy balance is possible, and the correlation length is $\lambda_E(E^*)$. If $\lambda_E(E)$ rapidly varies around E^*, two problems arise. First, the value of E achieving energy balancing:

$$E^*/\lambda_E(E^*) = \langle E/\lambda_E(E)\rangle = qF \quad \text{(A7)}$$

generally does not coincide with $\langle E\rangle$. Second, whereas the introduction of fluctuations in the Langevin manner was successful in a linear equation of motion such as (A2), it does not carry over to nonlinear systems. When the damping term $-E/\lambda_E$ is linear with respect to E, the superposition of a random force $f(x)$ averaging to zero does not induce any trouble. In the case of a *nonlinear* damping $-E/\lambda_E(E)$, the superposition of a random force is not possible if that force is linked to the damping. Now in our system $-E/\lambda_E(E)$ and $f(x)$ have the same physical origin, namely, the electron-lattice interaction. In Van Kampen's words,[40] $f(x)$ is an *internal* noise, and therefore the Langevin procedure is inapplicable. See Ref. 40 for a detailed account of the difficulties involved. In our case we simply admit the existence of an energy correlation length. The picture of lucky-drift flights suggests that autocorrelation of the energy breaks on the average at $l_c = E_{\rm av}/qF$ (see Sec. II C), but the small-signal linearized Langevin equation gives $l_c = \lambda_E(E^*)$. The example studied in Sec. II E shows that the second answer is right provided that the nonlinearity is not pronounced. Appreciable nonlinearity in the energy-balance equation is expected at intervalley transitions in direct-gap semiconductors, where the scattering time and hence $\lambda_E(E)$ sharply drop as a consequence of the increased density of available states. Other remarks can be found in Sec. II E.

[1] F. Capasso, in *Semiconductors and Semimetals,* edited by W. Tsang (Academic, San Diego, 1986), Vol. 22D, p. 1.
[2] P. A. Wolff, Phys. Rev. **95**, 1415 (1954).
[3] W. Shockley, Bell Syst. Technol. J. **30**, 990 (1951).
[4] W. Shockley, Solid-State Electron. **2**, 35 (1961).
[5] G. A. Baraff, Phys. Rev. **128**, 2507 (1962).
[6] B. K. Ridley, J. Phys. C **16**, 3373 (1983).
[7] W. Fawcett, A. D. Boardman, and S. Swain, J. Phys. Chem. Solids **31**, 1963 (1970).
[8] H. Shichijo and K. Hess, Phys. Rev. B **23**, 4197 (1981).
[9] Y.-C. Chang, D. Z.-Y. Ting, J. Y. Tang, and K. Hess, Appl. Phys. Lett. **42**, 76 (1983).
[10] M. V. Fischetti, IEEE Trans. Electron Devices **38**, 634 (1991).
[11] M. G. Burt, J. Phys. C **18**, L477 (1985).
[12] S. McKenzie and M. G. Burt, J. Phys. C **19**, 1959 (1986).
[13] P. A. Childs, J. Phys. C **20**, L243 (1987).
[14] B. K. Ridley and F. A. El-Ela, J. Phys. Condens. Matter **1**, 7021 (1989); Solid-State Electron. **32**, 1393 (1989).
[15] E. Bringuier, J. Appl. Phys. **70**, 4505 (1991).
[16] J. S. Marsland, R. C. Woods, and C. A. Brownhill, IEEE Trans. Electron Devices **39**, 1129 (1992).
[17] B. K. Ridley, Semicond. Sci. Technol. **2**, 116 (1987).
[18] E. A. Eklund, P. D. Kirchner, D. K. Shuh, F.R. McFeely, and E. Cartier, Phys. Rev. Lett. **68**, 831 (1992).
[19] L. Reggiani, in *Hot-electron Transport in Semiconductors,* edited by L. Reggiani, Topics in Applied Physics Vol. 58 (Springer-Verlag, Berlin, 1985), p. 7.
[20] C. Canali, F. Nava, and L. Reggiani, in *Hot-electron Transport in Semiconductors* (Ref. 19), p. 87.
[21] W. Shockley, J. A. Copeland, and R. P. James, in *Quantum Theory of Atoms, Molecules, and the Solid State,* edited by P.-O. Löwdin (Academic, New York, 1966), p. 537.
[22] S. McKenzie and M. G. Burt, Semicond. Sci. Technol. **2**, 275 (1987).
[23] K. Brennan, J. Appl. Phys. **64**, 4024 (1988).
[24] M. V. Fischetti, Phys. Rev. Lett. **53**, 1755 (1984); M. V. Fischetti, D. J. DiMaria, S. D. Brorson, T. N. Theis, and J. R. Kirtley, Phys. Rev. B **31**, 8124 (1985).
[25] E. O. Kane, Phys. Rev. **159**, 624 (1967).
[26] K. K. Thornber, J. Appl. Phys **52**, 279 (1981).
[27] S. M. Cho and H. H. Lee, J. Appl. Phys. **71**, 1298 (1992).
[28] C. L. Anderson and C. R. Crowell, Phys. Rev. B **5**, 2267 (1972).
[29] J. Bude and K. Hess, J. Appl. Phys. **72**, 3554 (1992).
[30] A. R. Beattie, Semicond. Sci. Technol. **7**, 401 (1992).
[31] M. Shen and X. Xu, Solid State Commun. **72**, 803 (1989).
[32] E. Cartier, M. V. Fischetti, E. A. Eklund, and F. R. McFeely, Appl. Phys. Lett. **62**, 3339 (1993).

[33]L. V. Keldysh, Zh. Eksp. Teor. Fiz. **37**, 713 (1959) [Sov. Phys. JETP **10**, 509 (1960)].
[34]A. R. Beattie, J. Phys. Chem. Solids **49**, 589 (1988).
[35]J. W. Allen, J. Phys. C **19**, 6287 (1986).
[36]H. E. Gumlich, J. Lumin. **23**, 73 (1981).
[37]U. Rössler, in *Intrinsic Properties of Group IV Elements and III-V, II-VI,* and *I-VII Compounds,* edited by O. Madelung, Landolt-Börnstein, New Series, Group III, Vol. 22, Pt. A (Springer, Berlin, 1988), pp. 168–171.
[38]E. Bringuier and A. Geoffroy, Appl. Phys. Lett. **60**, 1256 (1992).
[39]M. Beale, Philos. Mag. B **68**, 573 (1993).
[40]N.G. Van Kampen, *Stochastic Processes in Physics and Chemistry* (Elsevier, Amsterdam, 1981), Chap. VIII.